THE JOURNAL OF PHYSICAL CHEMISTRY B

Article

pubs.acs.org/JPCB

Binding of Fatty Acid Amide Amphiphiles to Bovine Serum Albumin: Role of Amide Hydrogen Bonding

Subhajit Ghosh and Joykrishna Dey*

Department of Chemistry, Indian Institute of Technology Kharagpur, Kharagpur 721 302, India

Supporting Information

ABSTRACT: The study of protein−surfactant interactions is important because of the widespread use of surfactants in industry, medicine, and pharmaceutical fields. Sodium *N*-lauroylsarcosinate (SL-Sar) is a widely used surfactant in cosmetics, shampoos. In this paper, we studied the interactions of bovine serum albumin (BSA) with SL-Sar and sodium *N*-lauroylglycinate (SL-Gly) by use of a number of techniques, including fluorescence and circular dichroism spectroscopy and isothermal titration calorimetry. The binding strength of SL-Sar is stronger than that of structurally similar SL-Gly, which differs only by the absence of a methyl group in the amide nitrogen atom. Also, these two surfactants exhibit different binding patterns with the BSA protein. The role of the amide bond and hence the surfactant headgroup in the binding mechanism is discussed in this paper. It was observed that while SL-Sar destabilized, SL-Gly stabilized the protein structure, even at concentrations less than the critical micelle concentration (cmc) value. The thermodynamics of surfactant binding to BSA was studied by use of ITC. From the ITC results, it is concluded that three molecules of SL-Sar in contrast to only one molecule of SL-Gly bind to BSA in one set of binding sites at room temperature. However, on increasing temperature four molecules of SL-Gly bind to the BSA through H-bonding and van der Waals interactions, due to loosening of the BSA structure. In contrast, with SL-Sar the binding process is enthalpy driven, and very little structural change of BSA was observed at higher temperature.

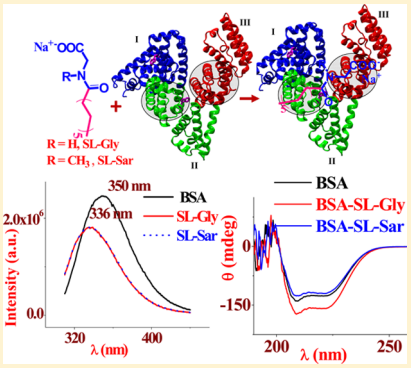

1. INTRODUCTION

Serum albumins (SAs) are the major (up to 40 g L^{-1}) constituent of blood plasma and not only play an important role in maintaining the osmotic pressure of the blood compartment[1,2] but also they serve as transporter protein for a variety of small molecules, including metabolites, endogenous and exogenous molecules, hormones, drugs, etc.[3−14] The SAs are well known to bind free fatty acids (FFA) and are the major vehicle for transport of fatty acids (FAs) in plasma.[15,16] In fact, the poor aqueous solubility of FAs is overcome by the presence of SA in plasma. Under normal physiological condition, 1 mol of human serum albumin (HSA) can carry around 0.1−2 mol of FA.[17] The FAs are also known to stabilize SA against denaturation.[16] It is now well established that the HSA has at least seven binding sites of varying affinities for FA molecules.[16,18] All FAs bind at site I in the same orientation with the carboxylate ($-COO^-$) group H bonded to Arg-117.[18] However, because of the complexity of the multiple binding interactions the structure of the HSA-FA complex is poorly understood. It has been found that long-chain FAs have a greater affinity for HSA in comparison to medium-chain FAs.[19,20] The binding affinity for HSA was also observed to increase with the increase of alkyl chain length of alkyl sulfate detergents.[21] On the basis of NMR studies of spin-labeled FA analogues and detergents, it has been suggested that hydrophobic interactions are the dominant mechanism by which FAs bind to the HSA.[22−24] However, methyl esters of the spin-labeled FA were observed to bind less tightly than the corresponding $-COO^-$ anion,[25] suggesting that electrostatic or hydrogen-bonding (H-bonding) interactions involving the carboxylate group also play a role in the FA binding to SA. The general view is that although hydrophobic interactions account for most of the binding energy, for large organic anions such as fatty acids an interaction occurs between the anions and certain positively charged residues, such as the ε-amino groups of lysine in the protein.[26] The role of electrostatic interaction is demonstrated by the weak binding of nonionic surfactants to the SA.[27,28]

The function of a protein generally depends upon its structure, and surfactant molecules are known to alter its structure and hence affect its functions including drug−protein interactions[29] and drug metabolizing enzyme activity.[30] Because of its relevance to the field of pharmaceutics protein−surfactant interactions have been the subject of extensive studies.[27,31−33] Most importantly, such studies can provide insight into the solubilizing[27,31] and renaturating[34,35] action of the surfactant on proteins. Bovine serum albumin (BSA) is one of the most studied proteins among SAs because of its (i) structural homology to the HSA, (ii) low cost, (iii) and high water solubility and (iv) it is easily available in pure form. BSA is a

Received: January 30, 2015
Revised: May 28, 2015
Published: May 29, 2015

DOI: 10.1021/acs.jpcb.5b00965
J. Phys. Chem. B 2015, 119, 7804−7815

heart-shaped protein consisting of 583 amino acid residues in a single polypeptide chain and has a molecular weight of 66 kDa.[36,37] It has three homologous domains (I, II, and III), each of which is further divided into two subdomains (IA, IB, etc.). The homologous domains are divided into nine loops by 17 disulfide bridges that make the heart-shaped structure of BSA more rigid.[38] As can be seen in Chart 1, BSA structure is

Chart 1. Structure of (a) BSA (PDB 3V03) and (b) HSA (PDB 1e7i)

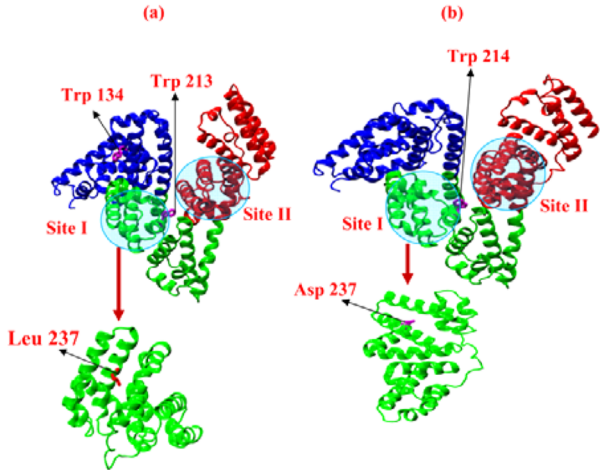

predominantly α-helical with the remaining polypeptide chain occurring in turns and flexible regions between subdomains with no β-sheets. Despite its structural homology to the HSA, BSA has only 75.8% of the biological functions of the former protein.[38,39] Structural analysis has shown that site II of BSA is similar to that of HSA. However, the site I of BSA (Chart 1a) is occupied by the Leu-237 residue compared to the hollow site I of HSA (Chart 1b). Therefore, it is expected that the Leu-237 residue in site I of BSA prevents the insertion of a hydrophobic molecule.

The study of BSA−surfactant interaction[40−43] in the bulk not only is important in industry but also is very important in the medical, cosmetic, and pharmaceutical fields. In fact, one of the most extensively studied systems is a BSA/SDS system.[44−49] SDS being a hard anionic surfactant causes skin irritation when it comes in contact with human skin. The reason for this skin irritation is the denaturation of the skin protein. Indeed, at a high surfactant concentration, the 3-D native structure of most globular proteins is destroyed, which is referred to as denaturation.[34,35,44,45,50−53] However, there are a few reports which show that SDS protects or stabilizes the BSA or HSA structure at very low concentrations from urea-[54] and thermal-induced[55,56] denaturation. Like SDS the double-tailed anionic surfactant, sodium bis(2-ethylhexyl) sulfosuccinate (AOT), at low concentrations also prevents decrement of the helicity of the HSA at higher temperatures, which establishes the protective nature of the surfactant.[57]

Currently, surfactants containing amide group are frequently used in industry. One of the commonly used surfactants is *N*-lauroylsarcosinate (SL-Sar) (see Chart 2 for structure). It is useful in making small-particle emulsions and suitable for cosmetics.[58] Also, it is used in toothpaste due to its good foaming property. Thus, it is an important component in making shampoos, bubble-bath pastes, washing creams, aerosols, etc. Moreover, it is well known as a reducing agent,

Chart 2. Chemical Structure of SL-Gly and SL-Sar Amphiphiles

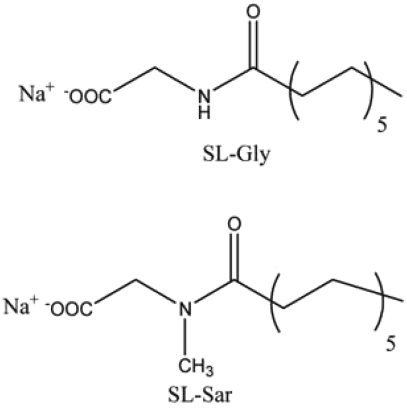

corrosion inhibitor, wetting, and flooding agent.[59,60] In the amide-containing surfactant, the amide group can act as a donor or an acceptor of H bonds. Indeed, amino acid-derived surfactants present a readily accessed source of electrostatic, H-bonding, and hydrophobic elements that are found in proteins. It has been demonstrated that the amino acid-terminated gold nanoparticles can effectively interact with positively charged proteins.[61] In a recent report[62] it has been observed that the morphology of the aggregate is different in *N*-lauroylglycinate (SL-Gly) and SL-Sar in water. The effect of the amide group of the amino acid-based surfactants in the aggregation process has also been reported by our group.[63−66] The only difference between these two surfactants is that the amide nitrogen is methylated in SL-Sar which converts the SL-Sar to an H-bond acceptor, but the absence of the methyl group makes the SL-Gly behave as both H acceptor and H donor. This means stronger intermolecular H bonding is possible in SL-Gly than in SL-Sar.

There are many reports where it is discussed that the binding of surfactant with BSA occurs mainly via hydrophobic interaction through the tail group and very little interaction through the headgroup. Therefore, in this work, it is intended to compare the mode as well as the efficiency of binding of SL-Gly and SL-Sar surfactants to BSA with those of FAs with comparable hydrocarbon chain length. Earlier studies reported the effect of the hydrocarbon chain length of FAs and detergents on protein−surfactant interaction.[60] However, the effect of the surfactant headgroup on its binding to proteins was not investigated systematically. The primary objective of the present study is to investigate the effect of the amide group in the surfactant headgroup on its binding to BSA. The difference in H-bonding ability of SL-Gly and SL-Sar is expected to alter their binding properties. Therefore, we examined the binding of SL-Sar and SL-Gly to BSA at concentrations much less than the respective critical micelle concentration (cmc) and also at different temperatures. In this investigation, we employed various methods, including steady-state and time-resolved fluorescence, circular dichroism (CD) spectroscopy, and isothermal titration calorimetry (ITC) for monitoring the BSA−surfactant interactions.

2. EXPERIMENTAL SECTION

2.1. Reagents. Lauroyl chloride and BSA were purchased from Sigma-Aldrich (St. Louis, MO). Sodium *N*-lauroylsarcosinate (SL-Sar) was purchased from Fluka and recrystallized

DOI: 10.1021/acs.jpcb.5b00965
J. Phys. Chem. B 2015, 119, 7804−7815

three times using ethanol/acetone (1:5 v/v) before use. Glycine was purchased from SRL (Mumbai). Warfarin was purchased from Chem Service (West Chester, PA), and ibuprofen was purchased from Alfa Aesar (England). All organic solvents, including tetrahydrofuran (THF), alcohol, acetone, and trimethyl amine (TEA), were purchased locally and used after purification and drying before use. Sodium *N*-lauroylglycinate (SL-Gly) was synthesized and purified by the literature reported method.[67] A 20 mM phosphate buffer of pH 7.0 was prepared in milli Q water (~18 MΩ), and all solutions were prepared using this buffer.

2.2. Sample Preparation. For all measurements, 15 μM (0.1%, w/v) BSA solutions in the buffer were prepared from the stock (0.4%, w/v) of BSA. One millimolar stock solution of the surfactants (SL-Sar and SL-Gly) was prepared in each case (exception was mentioned), and required amounts were added to the BSA solution to get the final solution. For warfarin, 5 mM stock was prepared in MeOH and then it was diluted to 10^{-4} M using buffer. Finally, a required amount of warfarin was added to the BSA solution to maintain the final concentration of 1.5×10^{-5} M. For ibuprofen, the same procedure is followed.

2.3. Surface Tension Measurements. The surface tension (γ) was applied to determine cmc by an automated surface tensiometer (model 3S, GBX, France) equipped with a thermostable vessel holder using the Du Nuöy ring detachment method. The temperature was maintained at 25 °C, and the platinum−iridium ring was carefully cleaned with 50% ethanol−HCl solution and finally with distilled water. The instrument was calibrated by measuring the γ of Mili-Q water (18.2 Ω). A stock solution of SL-Sar and SL-Gly was made in phosphate buffers (20 mM) of pH 7. The solutions were thoroughly mixed and allowed to equilibrate for 5 min before measurement.

2.4. Steady-State Fluorescence Measurements. Steady-state fluorescence measurements were carried out with a PerkinElmer LS-55 luminescence spectrometer equipped with a filter polarizer and a thermostats cell holder. The temperature was controlled using a circulating bath (Thermo Neslab, RTE 7). BSA concentration was kept at 15 μM, and SL-Sar and SL-Gly concentrations were varied. Phosphate buffer (20 mM) of pH 7 was used for preparing all solutions. A stock solution of 1 mM of each surfactant was prepared, an aliquot of which was used to make solutions of different concentrations. BSA solutions were excited at 295 nm, and the spectrum was recorded between 310 and 440 nm. The intensity was measured at the emission maximum (350 nm).

2.4.1. Stern−Volmer Quenching Study. The fluorescence quenching data were analyzed according to the Stern−Volmer (S−V) equation[68]

$$F_o/F = 1 + K_{S-V}[S] = 1 + k_q\tau_o[S] \quad (1)$$

where F_o and F are the fluorescence peak intensities (λ = 350 nm) of Trp in the absence and presence of surfactant (S), respectively, [S] is the added surfactant concentration, k_q is the bimolecular quenching rate constant, τ_o is the average lifetime of Trp in the absence of surfactant, and K_{S-V} is the S−V quenching constant.

2.4.2. Determination of BSA/Surfactant Binding Constants. On the assumption that there are n similar and independent binding sites[69] for a surfactant molecule S, in protein, P, the static quenching process can be represented as

$$nS + P \rightleftharpoons PS_n \quad (2)$$

$$K^n{}_b = \frac{[PS_n]}{[S]^n[P]} \quad (3)$$

where [S] and [P] are the surfactant and protein concentrations, respectively, and $[PS_n]$ is the concentration of the nonfluorescent fluorophore/quencher complex. Since fluorescence intensity is proportional to protein concentration one can write

$$[P]/[P]_o = F/F_o \quad (4)$$

$$[P] = F[P]_o/F_o \quad (5)$$

$$[S] = [S]_o - (F_o - F)[P]_o/F_o \quad (6)$$

$$[PS_n] = (F_o - F)[P]_o/F_o \quad (7)$$

where $[P]_o$ and $[S]_o$ are the total protein and surfactant concentrations, respectively. Substituting eqs 9−11 in eq 7 gives

$$K^n{}_b = \{(F_o - F)/F\}\{1/([S]_o - (F_o - F)[P]_o/F_o)\}^n \quad (8)$$

Therefore

$$\log\{(F_o - F)/F\} = n \log K_b - n \log\{1/([S]_o - (F_o - F)[P]_o/F_o)\} \quad (9)$$

2.5. Time-Resolved Fluorescence Measurements. For time-resolved fluorescence measurements, an Easy Life instrument from Optical Building Blocks Corp. was employed to measure the fluorescence lifetime of Trp residues of BSA. The light source was a 295 nm diode laser. A 305 nm emission cutoff filter was used to measure fluorescence signal. The time-resolved decay curves, after deconvolution of the instrument response function, were fitted to a biexponential function by an iterative technique. The data fitted well to a biexponential decay where the intensity is assumed to decay as the sum of individual single-exponential decay

$$I(t) = I(0)[a_1 e^{-t/\tau_1} + a_2 e^{-t/\tau_2}] \quad (10)$$

Here, $\tau_1$and τ_2 are the decay times and a_1 and a_2 are the amplitudes of the components at $t = 0$. The goodness of fit was evaluated by the reduced χ^2 (0.8−1.2) and weighted residuals as parameters. The average lifetime $\langle\tau_f\rangle$ was calculated by use of eq 2[68]

$$\langle\tau_f\rangle = f_1\tau_1 + f_2\tau_2 \quad (11)$$

where f_1 and f_2 are the fractional contribution to the total fluorescence intensity of the respective components. The BSA concentration in these experiments was kept fixed at 15 μM, and the SL-Gly and SL-Sar concentrations were both equal to 0.2 mM.

2.6. Circular Dichroism Spectra. A Jasco J-810 spectropolarimeter was used to measure the circular dichroism (CD) spectra using quartz cells of 1 mm path length. For each spectrum, an average of three scans was taken under the conditions of 1 nm band width, 2 s response time, and 50 nm/min scan speed. Each spectrum was baseline corrected using the appropriate reference solution. All measurements were carried out at 298 K. The spectrum was recorded in the range of 190−260 nm. An accumulation of three scans with a speed of 50 nm/min was performed, and data were collected. Now

DOI: 10.1021/acs.jpcb.5b00965
J. Phys. Chem. B 2015, 119, 7804−7815

the CD results are expressed in terms of the mean residue ellipticity (MRE) in deg cm^2 dmol^{-1}, which is defined as

$$\mathrm{MRE} = \theta_{obs}/(10 \times l \times C \times n) \quad (12)$$

where θ_{obs} is the circular dichroism in mdeg, l is the path length (0.1 cm), C is the molar concentration, and n is the number of amino acid residues (583). From the MRE value at 208 nm the percentage of α-helix content can be calculated using the following equation[70]

$$\alpha\text{-helix}(\%) = [(-\mathrm{MRE}_{208} - 4000)/(33\,000 - 4000)] \times 100 \quad (13)$$

where MRE_{208} is the observed MRE at 208 nm, 4000 is the value of β-form and random coil at 208 nm, and 33 000 is the value of pure α-helix conformation at 208 nm.

2.7. Isothermal Titration Calorimetry. Isothermal titration calorimetry (ITC) experiments were carried out in a Microcal iTC200 (made in the United States) at 298 K. Titration of surfactant against protein (BSA) was carried out by injecting 0.5 mM SL-Sar, 1 mM SL-Gly, and the same surfactant against phosphate buffer. BSA concentrations were kept at 15 μM in each case. The total number of injections was 20, and the cell temperature was 298 K. Reference power and initial delay were set to 5 and 60 s, respectively. A string speed of 600 rpm and spacing of 120 s were used for the ITC measurements.

The thermodynamic parameters for surfactant binding to BSA were estimated using the following equations

$$\Delta G^{\circ}_{b} = -RT \ln K_b \quad (14)$$

$$\Delta G^{\circ}_{b} = \Delta H^{\circ}_{b} - T\Delta S^{\circ}_{b} \quad (15)$$

where K_b is the binding constant, ΔH°_{b} is the standard enthalpy of binding, ΔS°_{b} is the standard entropy of binding, R is the gas constant, and T is the absolute temperature.

3. RESULTS AND DISCUSSION

3.1. cmc of Surfactants. As the pK_a of the corresponding N-acyl amino acid is ≤3.49,[71] both SL-Sar and SL-Gly exist in the carboxylate form at pH 7 and thus are expected to behave as anionic surfactant. The cmc values of SL-Sar and SL-Gly surfactants were determined in phosphate buffer (20 mM, pH 7) by surface tension measurements. The plots of variation of surface tension of phosphate buffer with the surfactant concentration are shown in Figure S1, Supporting Information. The concentration corresponding to the breakpoint in the plot was taken as the cmc value of the surfactant. The cmc values thus determined were 6.2 and 5.8 mM for SL-Sar and SL-Gly, respectively. The cmc values are less than those obtained in pure water,[72] which is due to increased counterion (Na^+) concentration in the buffer medium.

3.2. Fluorescence Spectroscopy. BSA has two tryptophan (Trp) residues in BSA: one in subdomain IB (Trp-134) and another in IIA (Trp-213). Trp-134 is located near the surface, and Trp-213 is located in the hydrophobic pocket of the protein (PDB 3V03)[73] Intrinsic fluorescence of BSA is due to these Trp residues. To examine whether the surfactant molecules bind to the BSA, the Trp fluorescence was measured in the presence of surfactant. The emission spectra of BSA in the absence and presence of 0.2 mM SL-Sar and SL-Gly surfactants are depicted in Figure 1. As seen BSA exhibits a strong emission band at λ_{max} = 350 nm when the excitation

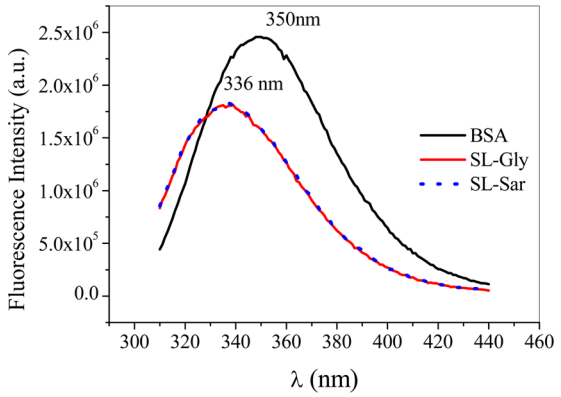

Figure 1. Fluorescence spectra of BSA in phosphate buffer (20 mM, pH 7) in the absence and presence of SL-Sar and SL-Gly surfactants (0.2 mM).

wavelength is fixed at 295 nm. It is found that the λ_{max} of the fluorescence emission band is shifted from 350 to 336 nm accompanied by a decrease of intensity upon surfactant addition to BSA solution, indicating interaction of the surfactant molecules with the protein. Similar spectral changes were also reported for FA binding to BSA, and two different processes were found to be responsible for the change of fluorescence properties.[74,75] It is well known that steady-state fluorescence spectra monitored the local microenvironment around the Trp residue. Since Trp fluorescence in nonpolar medium appears at lower wavelengths, the 335 nm emission can be associated with the Trp-213 residues buried in the hydrophobic pocket. However, the fluorescence emission of exposed Trp-134 appears at 350 nm due to solvent relaxation. The spectral shift can be due either to selective fluorescence quenching of the more solvent-exposed Trp-134 residue and/or to a conformational change in the protein. Since the CD spectral change as discussed below suggests a conformational change of the BSA, the blue shift in the fluorescence spectrum can be ascribed to the movement of the Trp-134 residue into an environment that is more protected from the solvent. This change, however, is secondary to structural changes associated with the surfactant binding at sites near the Trp-213 residue. The quenching of fluorescence can be associated with the alteration in the state of ionization of a ε-amino group in the protein, whereas the blue shift is attributed to the movement of Trp-134 residue into a less polar environment.[75] However, earlier studies suggested that the alkyl chain of the bound FA is located near Tyr residues, not the Trp residues.[76] In fact, there are numbers of strong FA binding sites located within 10 Å of the buried Trp-213 residue. However, there is no direct interaction of the alkyl chains bound at these sites with the Trp residue. The conformational change of BSA accompanied by surfactant binding to these sites alters the microenvironment of the buried Trp-213 residue, leading to fluorescence quenching as these strong binding sites are filled.

As shown in Figure S2, Supporting Information, the progressive decrease of fluorescence intensity of the Trp residue in the presence of surfactant may arise either as a result of dynamic quenching or as a result of conformational change in the protein induced by the surfactant binding (i.e., static quenching). The fluorescence quenching data of Trp residues were analyzed according to S−V eq 1. The S−V plots are presented in Figure 2, and the K_{S-V} values of different surfactants are listed in Table 1. The K_{S-V} value of SL-Gly is

DOI: 10.1021/acs.jpcb.5b00965
J. Phys. Chem. B 2015, 119, 7804−7815

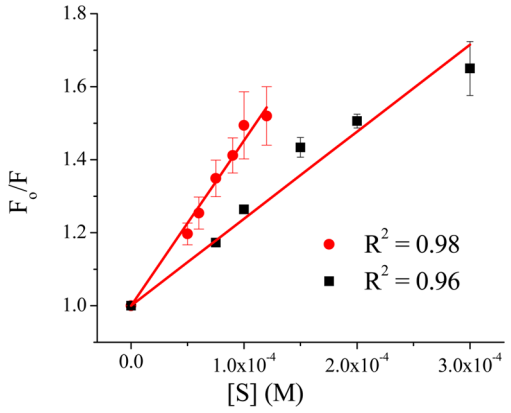

Figure 2. S−V plots of F_o/F vs [S] for (■) SL-Gly and (●) SL-Sar surfactants (S) in phosphate buffer (20 mM, pH 7.0) at 298 K.

smaller than that of the SL-Sar surfactant, suggesting a stronger interaction of the latter with BSA.

In order to estimate the values of k_q, the bimolecular quenching rate constant, we performed time-resolved fluorescence measurements. BSA fluorescence was observed to exhibit biexponential decay both in the absence and in the presence of surfactant. The representative fluorescence decay curves are shown in Figure S3, Supporting Information. The relevant decay data are compiled in Table 3. From the lifetime data of the Trp residue in BSA one can predict the degree of exposure of Trp to the aqueous phase. When the Trp residue is exposed to water its lifetime is greater than when it is in the hydrophobic environment. The average fluorescence lifetime ($\langle\tau_f\rangle$) of Trp in the absence of surfactant was taken as τ_o and used to calculate k_q (Table 1) from the respective K_{S-V} value. The data in Table 3 show that the τ_f value decreases when surfactant is added to the protein solution. The reduction of the τ_f value could be either due to dynamic quenching or a result of the conformational change of the protein structure which leads to a change of the microenvironment of Trp residues. The possibility of dynamic quenching can be ruled out because for both SL-Gly and SL-Sar; the quenching constants are on the order of $\sim 10^{11}$ M^{-1} s^{-1}, which is much higher than the maximum limit (2×10^{10} M^{-1} s^{-1})[77] of k_q for a diffusion-controlled bimolecular reaction. Therefore, the decrease of τ_f value must be due to the conformational change of BSA structure as a result of surfactant binding, which is also evident from the change of the CD spectrum discussed below.

In support of the above conclusion, we also measured the K_{SV} at different temperatures for both BSA/SL-Sar and BSA/SL-Gly systems. Figures S4 and S5, Supporting Information, show the S−V plots of the BSA/SL-Sar and BSA/SL-Gly systems at different temperatures. The relevant data are collected in Table 2. It is observed from the data in Table 2 that the K_{SV} value decreases with increasing temperature for both systems. This suggests that the fluorescence quenching is static in nature, and the respective K_{S-V} value can be treated as the apparent value of the association (or binding) constant

Table 2. K_{S-V} Values of SL-Gly and SL-Sar Measured in Phosphate Buffer (20 mM, pH 7) at Different Temperatures

	$K_{S-V} \times 10^{-3}$ M^{-1}		
surfactant	293 K	298 K	303 K
SL-Sar	5.49 ± 0.14	4.52 ± 0.11	3.68 ± 0.14
SL-Gly	3.93 ± 0.14	2.38 ± 0.12	2.10 ± 0.08

(K_b) of the surfactant. As the τ_f value of both Trp residues decreases upon interaction with the surfactant, one can conclude that the Trp-134 residue on the protein surface is going to the more hydrophobic environment relative to that in native BSA. However, simultaneous binding to the hydrophobic pocket containing the Trp-213 residue cannot be ruled out. Indeed, the decrease of fluorescence lifetime of both components in the presence of surfactant indicates this. This is further substantiated by the results of site-competitive experiments described below.

3.3. Determination of Binding Site Using Site Markers. The site marker experiment is a very useful technique to determine the binding pocket of BSA. Warfarin is a site marker and binds to BSA in subdomain IIA, which is the drug binding site I. Since warfarin is a hydrophobic drug, when it binds to BSA, its fluorescence intensity is enhanced relative to that in water. However, the fluorescence intensity is gradually quenched upon addition of SL-Gly (Figure S6, Supporting Information) or SL-Sar (Figure S7, Supporting Information) surfactant to the warfarin-bound BSA solution. When SL-Gly or SL-Sar (0.2 mM) was added to the warfarin-bound BSA solution, the warfarin fluorescence is almost completely quenched to that observed in buffer (Figure 3). This site-competitive experiment clearly suggests that both SL-Sar and SL-Gly displace warfarin from the site I of BSA.

A similar experiment was also carried out using ibuprofen, which is a site II binder of BSA in subdomain IIIA. In order to determine whether SL-Gly and SL-Sar bind to Sudlow's site II or not, the ibuprofen-bound protein was titrated using both SL-Gly and SL-Sar surfactants by monitoring Trp fluorescence in phosphate buffer at room temperature. The S−V plots (Figure 4) were then constructed according to eq 5. The value of S−V quenching constant (K'_{S-V}) in the presence of ibuprofen was determined from the slope of the respective S−V plot. The K'_{S-V} values thus obtained (Table 1) are 3.51×10^3 and 1.66×10^3 M^{-1} for SL-Sar and SL-Gly, respectively, and can be taken as the binding constants for site I. However, it is observed that the K'_{S-V} value is less than the corresponding K_{S-V} value (Table 1), which means the binding affinity of the surfactants to site I of BSA is not independent of binding to site II. From this we can conclude that both SL-Gly and SL-Sar bind to site I as well as site II. This means both surfactants simultaneously bind to subdomain IIA and subdomain IIIA of the protein.

3.4. BSA/Surfactant Binding Constants. According to eq 9, a plot of $\log[(F_o - F)/F]$ vs $\log\{1/([S]_o - [P]_o(F_o - F)/F_o)\}$ should produce a straight line with slope n and intercept $n \log K_b$. The plots in Figure 5 show a good linear relationship

Table 1. Values of K_{S-V}, k_q, K'_{S-V}, K_b, and n for the Binding of SL-Gly and SL-Sar with BSA in Phosphate Buffer (20 mM, pH 7) at Room Temperature

	$K_{S-V} \times 10^{-3}$ M^{-1}	$k_q \times 10^{-11}$ M^{-1} s^{-1}	$K'_{S-V} \times 10^{-3}$ M^{-1}	$K_b \times 10^{-3}$ M^{-1}	n
SL-Sar	4.52 ± 0.11	8.69 ± 0.96	3.84 ± 0.16	5.62 ± 0.20	1.19 ± 0.06
SL-Gly	2.38 ± 0.12	4.58 ± 0.71	1.80 ± 0.05	2.51 ± 0.23	0.96 ± 0.10

DOI: 10.1021/acs.jpcb.5b00965
J. Phys. Chem. B 2015, 119, 7804−7815

Table 3. Fluorescence Lifetime (τ/ns), Average Lifetime ($\langle\tau_f\rangle$/ns), Fractional Intensity (f), and Associated Parameters of BSA and BSA/Surfactant Complex in Phosphate Buffer (20 mM, pH 7) at 298 K

substances	τ_1	τ_2	f_1	f_2	χ^2	$\langle\tau_f\rangle$
BSA	5.42 ± 0.10	2.32 ± 0.06	0.942 ± 0.004	0.0583 ± 0.002	1.068	5.2 ± 0.1
BSA/SL-Sar	3.88 ± 0.19	1.99 ± 0.06	0.866 ± 0.027	0.136 ± 0.026	1.077	3.6 ± 0.2
BSA/SL-Gly	3.97 ± 0.21	1.88 ± 0.11	0.890 ± 0.014	0.110 ± 0.013	0.925	3.7 ± 0.2

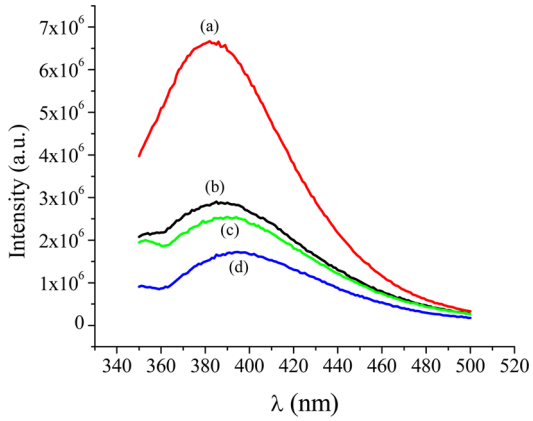

Figure 3. Fluorescence spectra of warfarin and warfarin-bound BSA in buffer in the presence and absence of 0.2 mM surfactant: (a) BSA/warfarin, (b) BSA/warfarin/SL-Gly, (c) BSA/warfarin/SL-Sar, and (d) warfarin, λ_{ex} = 325 nm.

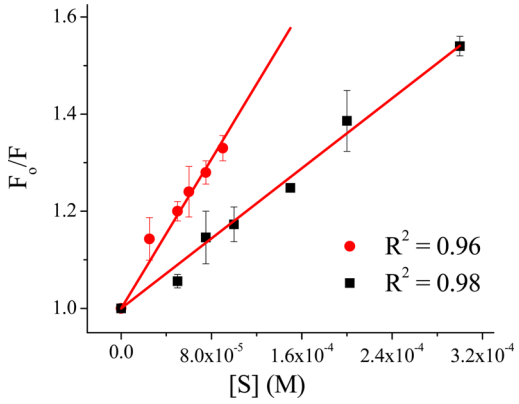

Figure 4. S−V plots for the interactions of (■) SL-Gly and (●) SL-Sar with ibuprofen-bound BSA in phosphate buffer (20 mM, pH 7) at room temperature.

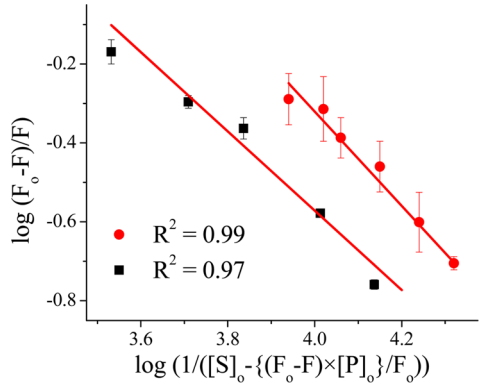

Figure 5. Plot of $\log[(F_o - F)/F]$ vs $\log\{1/([S]_o - [P]_o(F_o - F)/F_o)\}$ for (■) SL-Gly and (●)SL-Sar surfactants in phosphate buffer (20 mm, pH 7.0) at 298 K.

between $\log[(F_o - F)/F]$ and $\log\{1/([S]_o - [P]_o(F_o - F)/F_o)\}$. The binding constant was obtained from the intercept, and the data are collected in Table 1. For both surfactants, the value of n is found to be close to 1.0, indicating surfactant binding to just a single binding site in BSA. Thus, the SL-Sar and SL-Gly surfactants are most likely to bind to the hydrophobic pocket in subdomain IIA where Trp-213 is located. This is in contrast to FAs that are known to have at least two binding sites (sites I and II) where they bind BSA more tightly and a few nonspecific binding sites where binding is weaker. Of the three homologous domains the surfactant molecules bind only to the fatty acid binding sites I and II. Therefore, the surfactant molecule might be bound to the BSA in such a way that the hydrophobic tail is inserted into the hydrophobic pocket of the subdomain IIA of BSA and the polar carboxylate headgroup falls into the ibuprofen binding site in the subdomain IIIA. This results in a decrease of micropolarity of both Trp-213 and Trp-134 residues as manifested by the blue-shifted fluorescence emission spectrum of BSA upon surfactant binding. On the other hand, it is also possible that the surfactant molecules bind to the hydrophobic pocket in subdomain IIA, where Trp-213 is located and triggers a conformational change of the protein structure which in turn pushes the Trp-134 residue to a less polar environment. Indeed, the conformational change of the protein is manifested by the change in the CD spectrum of the native BSA upon surfactant addition.[78]

The binding constants obtained for the BSA/surfactant systems suggest low affinity binding compared to BSA/FA complexes.[16,79,80] However, their interactions are comparable to other anionic surfactants, such as SDS (2×10^3 M^{-1}).[81] It is interesting to note that the binding constant of \ SL-Sar is almost double that of \ SL-Gly, which means the binding efficiency of the former surfactant is higher than that of the latter. The higher binding constant of \ SL-Sar can be easily explained by considering the structure of the SL-Sar surfactant. As the *N*-methyl group in the surfactant makes the headgroup more hydrophobic and hence less hydrated, the binding of the headgroup to \ site II is facilitated, thus increasing the value of the binding constant. However, in the case of SL-Gly, the unsubstituted amide linkage makes the headgroup more polar, thus facilitating stronger interaction with bulk water, thereby reducing its binding efficiency to site II. In fact, the binding efficiency of both SL-Gly and SL-Sar is much less than the corresponding fatty acid,[79] which is much less soluble in water.

3.5. Conformational Changes upon Surfactant Binding. Circular dichroism (CD) is a powerful tool to determine the protein secondary and tertiary structure. If the binding of ligand to BSA is accompanied by conformational changes, it can be easily monitored by CD spectra. The CD spectrum (Figure 6a and 6b) of BSA consists of two minima corresponding to the $\pi-\pi^*$ and n−π^* transition at 208 and 222 nm, respectively, due to the helicity of the peptide chain. The CD spectra of BSA in the presence different concentrations of SL-Gly (Figure 6a) and SL-Sar (Figure 6b) were also measured. The change in the CD

DOI: 10.1021/acs.jpcb.5b00965
J. Phys. Chem. B 2015, 119, 7804−7815

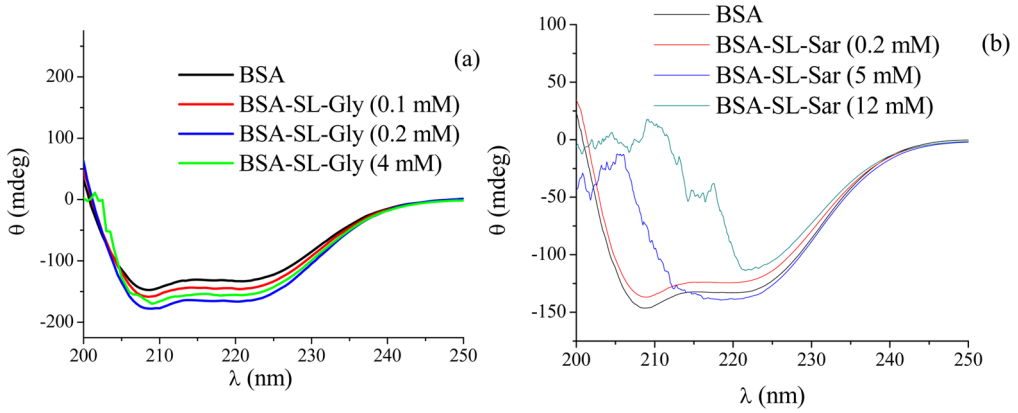

Figure 6. CD spectra of BSA in the presence of different concentrations of (a) SL-Gly and (b) SL-Sar in phosphate buffer (20 mM, pH 7) at 298 K.

spectrum clearly suggests a conformational change of the protein. It can be observed that despite the similar structure the effect of surfactant binding is different with SL-Sar and SL-Gly. It is observed that at very low concentrations, binding of SL-Sar caused a slight decrease of the intensity of the CD band. However, at higher surfactant concentrations (>5 mM) of the SL-Sar the peak corresponding to 208 nm slowly disappears, which means that the BSA denaturation starts before the cmc of the SL-Sar. When the concentration of SL-Sar was increased to 12 mM it was found that the 208 nm peak disappeared, but there was no shift of the peak at 222 nm, which corresponds to β-sheet and random coil structure of the protein. In contrast, with SL-Gly first stabilization occurs at low concentrations ($\leq$0.2 mM) as indicated by the increase of intensity of the CD band, but upon further increase of concentration the BSA structure is destabilized.

The CD spectra were analyzed using the CONTIN analysis program obtained from dichroweb. The relevant data are listed in Table S1, Supporting Information. Unfortunately, the analysis failed to give reliable results as the CD spectra below 200 nm were noisy. Therefore, we calculated the percentage of α-helix structure using eq 13. In the native state, α-helix percentage is 43.07% (see Table 4), which is very close to those

Table 4. Contents of α-Helix Structure in BSA and in BSA/Surfactant Complexes in Phosphate Buffer (20 mM, pH 7) at Room Temperature ([SL-Sar] = [SL-Gly] = 0.2 mM)

substance	BSA	BSA/SL-Sar	BSA/SL-Gly
% of α-helix	43.07 ± 1.07	37.81 ± 2.17	58.33 ± 4.33

reported by others.[82] The α-helix percentage, however, decreased to 37.81% upon addition of 0.2 mM SL-Sar, indicating destabilization of the protein structure. In contrast, upon addition of the same concentration of SL-Gly the α-helix percentage increased to 58.33%, indicating stabilization of the protein structure. Since both surfactants have similar chain length, the opposite behavior can be attributed to the difference in their headgroup structures. The presence of a methyl group in the amide nitrogen increases the headgroup hydrophobicity of SL-Sar compared to SL-Gly, leading to tighter binding to BSA and hence destabilization of the protein structure.

3.6. Thermodynamics of Surfactant Binding. The driving forces for binding of ligands to proteins usually involve H-bonding, van der Waals, electrostatic, and/or hydrophobic interactions. In order to understand the nature of interactions between BSA and SL-Sar (or SL-Gly), thermodynamic parameters were calculated from the data obtained from ITC measurements. ITC measurement is one of the most sensitive techniques that permits direct measurement of changes of the thermodynamic parameters in the course of binding of surfactant to protein. The binding process can be fully understood by the contribution of enthalpy and entropy from protein, ligand, and the solvent water.[83] Here, 15 μM BSA was titrated by 1 mM SL-Gly or 0.5 mM SL-Sar. Each injection exhibits the exothermic nature of the binding. The binding isotherms of SL-Sar and SL-Gly are shown in Figure 7a and 7b. As can be seen from the plots, the two protein/surfactant systems exhibit distinctly different heat change profiles. The heat changes were fitted to isothermal functions in order to quantify the corresponding thermodynamic parameters. For both SL-Sar and SL-Gly the data can only be fitted to a mode of a single set of identical binding sites. The binding constants (K_b), enthalpy changes (ΔH°_b), and binding stoichiometry (n) were obtained from respective titration curves. The Gibbs free energy changes (ΔG°_b) and entropy changes (ΔS°_b) were calculated using eqs 14 and 15, respectively. The values of the thermodynamic parameters for the protein/surfactant systems are summarized in Table 5.

Examination of the thermodynamic data listed in Table 5 shows that ΔG°_b values for both surfactants are negative, which means complex formation with BSA for both surfactants is spontaneous. The binding constant of SL-Sar is greater than that of SL-Gly and consistent with the results obtained from fluorescence studies. However, K_b values obtained from ITC measurements are greater than the respective value obtained from fluorescence measurements. The complexation of SL-Sar as well as SL-Gly surfactant with BSA is exothermic. However, in contrast to the results of fluorescence measurements, the surfactants exhibit drastically different binding stoichiometry with BSA, which depends on the headgroup structure. This might be because of the fact that fluorescence is an indirect method, whereas ITC is a direct method of binding studies. From the enthalpic viewpoint, the formation of noncovalent bonds is exothermic. For both surfactants, the major contribution to ΔG°_b comes from the ΔH°_b term, suggesting that the protein−surfactant interaction is electrostatic and/or H bonding in nature. In the case of SL-Sar, the ΔH°_b value (-25.22 kJ mol^{-1}) is slightly offset by the small positive ΔS°_b value (18.39 J K^{-1} mol^{-1}), which means, electrostatic interaction is the main driving force for stabilization of BSA/SL-Sar complex. The enthalpy change in removal of water

DOI: 10.1021/acs.jpcb.5b00965
J. Phys. Chem. B 2015, 119, 7804−7815

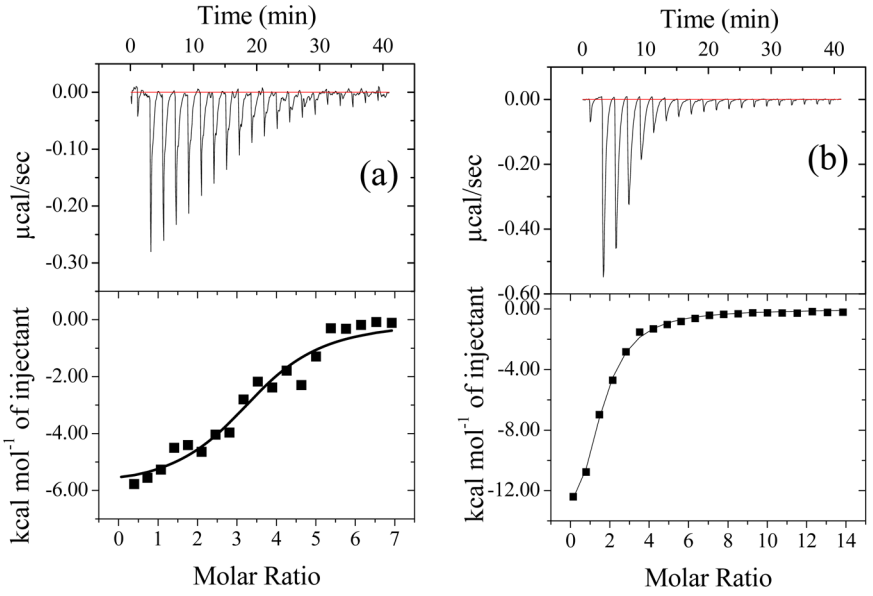

Figure 7. ITC plots of surfactant binding with BSA in phosphate buffer (20 mM, pH 7) at 298 K: (a) SL- Sar and (b) SL-Gly.

Table 5. Thermodynamic Parameters of BSA−Surfactant Interactions Obtained from ITC Measurements in Phosphate Buffer (20 mM, pH 7) at 298 K

surfactant	ΔH°_b (kJ mol^{-1})	ΔS°_b (J K^{-1} mol^{-1})	ΔG°_b (kJ mol^{-1})	K_b (M^{-1})	n
SL-Sar	−25.22 ± 1.72	18.39	−30.70	2.28 × 10^5 ± 7.90 × 10^4	3.43 ± 0.16
SL-Gly	−80.76 ± 3.64	−174.72	−28.69	1.02 × 10^5 ± 8.50 × 10^3	1.31 ± 0.05

Table 6. Binding Number (n), Enthalpy of Binding (ΔH°), Entropy of Binding (ΔS°), and Binding Constant (K) for the Interaction of BSA with SL-Sar and BSA−SL-Gly in Phosphate Buffer (20 mM, pH 7) at Different Temperatures

surfactant		298 K	303 K	308 K
	n	3.43 ± 0.16	3.28 ± 0.11	3.81 ± 0.22
SL-Sar	ΔH° (kJ mol^{-1})	−25.22 ± 1.72	−27.87 ± 1.33	−34.15 ± 3.31
	ΔS° (J K^{-1} mol^{-1})	18.39	10.37	−17.43
	K (M^{-1})	2.28 × 10^5 ± 7.90 × 10^4	2.12 × 10^5 ± 4.96 × 10^4	7.25 × 10^4 ± 2.17 × 10^4
SL-Gly	ΔH_1° (kJ mol^{-1})	−80.76 ± 3.64	−135.20 ± 10.87	−211.76 ± 54.18
	ΔS_1° (J K^{-1} mol^{-1})	−174.72	−340.20	−588.00
	K_1 (M^{-1})	1.02 × 10^5 ± 8.50 × 10^3	3.17 × 10^5 ± 1.2 × 10^5	1.29 × 10^5 ± 8.8 × 10^4
	ΔH_2° (kJ mol^{-1})		86.39 ± 11.84	290.38 ± 162.54
	ΔS_2° (J K^{-1} mol^{-1})		397.74	1041.60
	K_2 (M^{-1})		7.32 × 10^5 ± 5.3 × 10^5	1.63 × 10^5 ± 1.2 × 10^5
	ΔH_3° (kJ mol^{-1})		−93.32 ± 7.98	−151.45 ± 146.58
	ΔS_3° (J K^{-1} mol^{-1})		−220.5	−380.94
	K_3 (M^{-1})		3.49 × 10^4 ± 9.3 × 10^3	5.51 × 10^5 ± 5.3 × 10^5
	ΔH_4° (kJ mol^{-1})			−121.92 ± 23.18
	ΔS_4° (J K^{-1} mol^{-1})			−309.12
	K_4 (M^{-1})			3.27 × 10^4 ± 1.5 × 10^4

molecules from the BSA cavity (which is negative in sign) and destruction of the iceberg structure of the surfactant (which is positive in sign) contributes to the net enthalpy change of the BSA−SL-Sar interaction. Since the overall enthalpy change is negative, the former value exceeds the latter value. The small positive value of ΔS, on the other hand, indicates hydrophobic interaction that stabilized the complex. The contributing factors to the net entropy are (i) removal of water from the iceberg, (ii) removal of water from the binding site of BSA, and (iii) association of BSA with SL-Sar. As the former two contributions are positive and that of the latter one is negative, the former two contributions exceed the latter one, indicating that SL-Sar binding is accompanied by removal of water from the binding site. This means that the surfactant binding to BSA is through the headgroup that binds electrostatically to site II as well as through the tail that is inserted into the hydrophobic cavity near the Trp-213 residue. According to the data presented in Table 1, three molecules of SL-Sar bind to the BSA. If the first molecule of SL-Sar binds to the hydrophobic pocket then there must be two other sites elsewhere in BSA where the other two molecules can bind. It is reported that the fatty acids first bind to BSA in the high-affinity binding site I and also to two other high-affinity binding sites.[25]

For SL-Gly also we observed a similar binding mechanism in which the molecule binds to BSA through electrostatic and/or H-bonding and van der Waals interactions. The negative ΔH

DOI: 10.1021/acs.jpcb.5b00965
J. Phys. Chem. B 2015, 119, 7804−7815

value (−80.76 kJ mol^{-1}) for the binding is found to be very large compared to that for SL-Sar surfactant, suggesting stronger H-bonding interaction in the case of SL-Gly. This is expected as SL-Gly can act as H-bond donor as well as acceptor. The ΔS value (−174.72 J K^{-1} mol^{-1}) is also observed to be very large and negative for the binding and can be attributed to tighter association of SL-Gly with BSA. However, the ΔH value overweighs the entropy gain due to release of water molecules from the cavity and/or iceberg. Thus, it is concluded that the amide bond in the surfactant headgroup plays an important role in determining the binding mode of the surfactant molecule.

3.7. Effect of Temperature on Binding of Surfactant. To get better insight into the nature of binding of BSA−surfactants we measured the thermodynamic parameters at different temperatures (see Table 6). For SL-Sar the binding is hydrophobic in nature, but weak H bonding seems to help in forming the complex. Due to the presence of a methyl group in the amide nitrogen the H-bonding ability of SL-Sar decreases. The H bonding occurs through the $-COO^-$ group in SL-Sar. When the temperature is slightly increased the H-bonding and van der Waals interactions become more important for the formation of the BSA/surfactant complexes. Indeed, the increase of the negative $\Delta H°$ value suggests that for the BSA/SL-Sar system the major driving force is not a H-bonding but an electrostatic interaction. For SL-Sar, both the binding constant (K) and ΔS decrease with increasing temperature, which means the process is enthalpy driven. However, the ΔC_P value as obtained from the slope of the plot of $\Delta H°$ vs T (Figure 8) for the BSA/SL-Sar system (− 760 J K^{-1} mol^{-1}) is

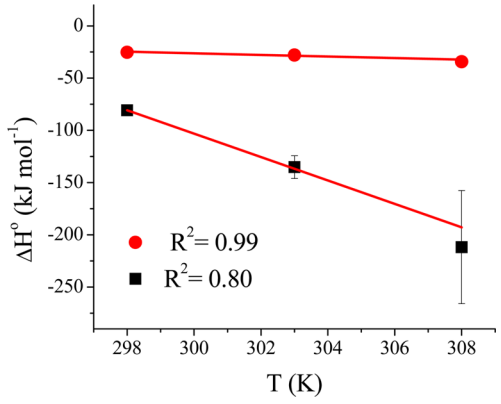

Figure 8. Plot of $\Delta H°$ vs temperature (T/K) for (■) SL-Gly and (●) SL-Sar surfactants.

negative, indicating that only a small structural change involving burial of the hydrophobic groups of the protein occurs with the increase of temperature.

On the other hand, for SL-Gly with increasing temperature the association process changes from single-step binding to sequential binding mode. Indeed, at 308 K the binding occurs in four sequential steps with four different values of each of K (K_1, K_2, K_3, K_4), $\Delta H°$ ($\Delta H°_1$, $\Delta H°_2$, $\Delta H°_3$, $\Delta H°_4$), and $\Delta S°$ ($\Delta S°_1$, $\Delta S°_2$, $\Delta S°_3$, $\Delta S°_4$). At 298 K, the association process is enthalpy driven and H bonding is the main driving force for forming the complex, but with increasing temperature the H-bonding interaction becomes more favorable as the values of both $\Delta H°$ and $\Delta S°$ become more negative (see Table 6). With increasing temperature loosening of BSA structure occurs, which helps binding of more molecules of SL-Gly sequentially with BSA. At temperatures of 303 and 308 K, SL-Gly shows positive cooperativity, that is, after the binding of the first molecule, the second and third molecule easily binds to BSA. Interestingly, at 308 K, the binding constant of the forth molecule is less than that of the third one, showing negative cooperativity. However, for the BSA/SL-Gly system, the ΔC_P value is −11.21 kJ K^{-1} mol^{-1}, which is quite large and indicates burial of hydrophobic groups upon surfactant binding. This means stabilization of the BSA structure upon surfactant binding as also supported by the CD spectral data.

To further support the effect of temperature on the stability of BSA−surfactant complex, we studied the temperature-induced unfolding (see Figures S8 and S9, Supporting Information) of BSA/surfactant complex of both surfactants using CD spectroscopy. The T_m values obtained from the respective titration curve show that the T_m value of pure BSA (55 °C) is shifted to 70 °C in the presence of both SL-Gly and SL-Sar. This means that both surfactants stabilize the BSA structure. From Figure S9, Supporting Information, it is very clear that initially due to the tighter binding of SL-Sar to BSA the protein attains a partially unfolded structure which favors simultaneous binding of the surfactant molecule in the two domains (IIA and IIIA) of BSA, thereby making the protein structure more rigid. Consequently, the T_m value is increased.

3.8. Effect of Ionic Strength on Binding of Surfactant. At pH 7.0, the BSA molecule has a net charge of −18, which is distributed as −10 in the domain I and −8 in domain II.[12] The value of the binding constant is expected to decrease with an increase in the ionic strength. If the association of the surfactant in the protein binding cavity involves electrostatic interactions since the ions of salt will also compete for binding to the charged residues. To test the role of electrostatic interaction in the binding of the BSA−SL-Sar system we increased the ionic strength of the solution by increasing the buffer concentration from 5 to 50 mM. However, the plots in Figure 9 show that the

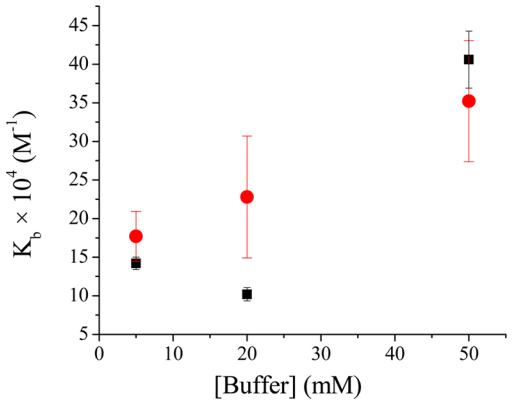

Figure 9. Plot of K_b vs [Buffer] for the interactions of BSA with SL-Gly (■) and SL-Sar (●) surfactants in phosphate buffer (pH 7.0) at 298 K.

binding constant increases with increasing buffer concentration. This means BSA−SL-Sar binding is mainly hydrophobic in nature as already concluded from the thermodynamic binding data. In the case of the BSA/SL-Sar system the binding constant is linearly increased with the PBS concentration, whereas in the case of the BSA/SL-Gly system a nonlinear change of K_b is observed. This may be due to the higher polarity of the Gly headgroup. Due to the presence of the hydrophobic tail in SL-Gly the hydrophobic effect could not be

DOI: 10.1021/acs.jpcb.5b00965
J. Phys. Chem. B 2015, 119, 7804−7815

neglected. Therefore, a combination of hydrophobic and polar interactions is responsible for the binding of SL-Gly to BSA, which is reflected by the K_b values shown in Figure 9.

4. CONCLUSIONS

In summary, we studied the interaction of sodium *N*-lauroylsarcosinate (SL-Sar), a widely used surfactant in cosmetics and shampoos, with bovine serum albumin (BSA), and the results were compared with those of sodium *N*-lauroylglycinate (SL-Gly). The effect of headgroup structure on surfactant binding was investigated. Like fatty acids (FAs), upon increasing the concentration of SL-Sar and SL-Gly both surfactants were observed to quench protein fluorescence, indicating binding of the surfactant molecules to the protein. However, the nature of binding differs markedly from those of FAs. For both SL-Sar and SL-Gly, the surfactant molecules were observed to exhibit noncooperative binding as evidenced by the lowering of the binding constant (K_b) and free energy of binding (ΔG_b°) values in comparison to FAs. In contrast to FAs which have six binding sites in BSA, a set of three sites for SL-Sar and only one binding site for SL-Gly were observed. These surfactant molecules were observed to bind to the warfarin binding site I located in the hydrophobic cleft between two lobes of the protein structure as well as to the ibuprofen binding site II. The binding to site I is hydrophobic in nature for both surfactants. Interestingly, the binding to site II is electrostatic for SL-Sar but tight H bonding in the case of SL-Gly. However, the binding constant for SL-Sar is almost double that of SL-Gly. Since the *N*-methyl group in the surfactant makes the headgroup more hydrophobic and hence less hydrated, the binding of the headgroup to site II is facilitated as manifested by the higher value of the binding constant. Thus, it is concluded that the amide bond in the surfactant headgroup plays an important role in determining the binding mode of the surfactant molecule, and consequently, the binding pattern is different for SL-Sar and SL-Gly. Although the higher binding affinity of SL-Sar causes initial unfolding of the protein, both SL-Gly and SL-Sar exhibit stabilization of the BSA native structure in the low concentration range.

It is interesting to note that upon increasing temperature more molecules of SL-Gly bind to BSA through H-bonding and van der Waals interactions, which means loosening of the BSA structure at higher temperatures. The large negative ΔC_p value ($-$ 11.21 kJ K^{-1} mol^{-1}) of the BSA/SL-Gly system clearly suggests a large change in the BSA structure involving burial of the hydrophobic groups with the increase of temperature. In contrast, with SL-Sar, both K and ΔS decrease with increasing temperature, which means the process is enthalpy driven. However, the ΔC_p value for the BSA/SL-Sar system ($-$ 760 J K^{-1} mol^{-1}) is much less negative compared to that of the BSA/SL-Gly system, indicating only a small structural change of the protein occurs upon binding of SL-Sar.

■ ASSOCIATED CONTENT

Supporting Information

Surface tension plots, fluorescence spectra of BSA in the presence of SL-Gly and SL-Sar, fluorescence decay plots, S–V plot of SL-Gly and SL-Sar at different temperatures, fluorescence spectra of warfarin and warfarin-bound BSA in the presence and absence of SL-Sar and SL-Gly, and CD spectra of surfactant-bound BSA at different temperatures. The Supporting Information is available free of charge on the ACS Publications website at DOI: 10.1021/acs.jpcb.5b00965.

■ AUTHOR INFORMATION

Corresponding Author

*Fax: (+) 91-3222-255303. E-mail: joydey@chem.iitkgp.ernet.in.

Notes

The authors declare no competing financial interest.

■ ACKNOWLEDGMENTS

We thank the Indian Institute of Technology Kharagpur for partial support of this work. S.G. thanks UGC, New Delhi. for a research fellowship.

■ REFERENCES

(1) Moriyama, Y.; Ohta, D.; Hachiya, K.; Mitsui, Y.; Takeda, K. Fluorescence behavior of tryptophan residues of bovine and human serum albumins in ionic surfactant solutions: A comparative study of the two and one tryptophan(s) of bovine and human albumins. *J. Protein Chem.* **1996**, *15*, 265–272.

(2) Ercelen, S.; Klymchenko, A. S.; Mely, Y.; Demchenko, A. P. The binding of novel two-color fluorescence probe FA to serum albumins of different species. *Int. J. Biol. Macromol.* **2005**, *35*, 231–242.

(3) Peters, T. *All About Albumin: Biochemistry, genetics, and Medical Applications*; Academic: San Diego, 1996.

(4) Choi, J. K.; Ho, J.; Curry, S.; Qin, D.; Bittman, R.; Hamilton, J. A. Interactions of very long-chain saturated fatty acids with serum albumin. *J. Lipid Res.* **2002**, *43*, 1000–1010.

(5) Makino, S.; Reynolds, J. A.; Tanford, C. The binding of deoxycholate and Triton X-100 to proteins. *J. Biol. Chem.* **1973**, *248*, 4926–4932.

(6) Zhang, Y.; Wilcox, D. E. Thermodynamic and spectroscopic study of Cu(II) and Ni(II) binding to bovine serum albumin. *J. Biol. Inorg. Chem.* **2002**, *7*, 327–337.

(7) Kamikubo, K.; Sakata, S.; Nakamura, S.; Komaki, T.; Miura, K. Thyroxine binding to human serum albumin immobilized on sepharose and effects of nonprotein albumin-binding plasma constituents. *J. Protein Chem.* **1990**, *9*, 461–465.

(8) Sengupta, B.; Sengupta, P. K. The interaction of quercetin with human serum albumin: A fluorescence spectroscopic study. *Biochem. Biophys. Res. Co.* **2002**, *299*, 400–403.

(9) Feng, X. Z.; Liu, Z.; Yang, L. J.; Wang, C.; Bai, C. L. Investigation of the interaction between acridine orange and bovine serum albumin. *Talanta* **1998**, *47*, 1223–1229.

(10) Olson, R. E.; Christ, D. D. Chapter 33. Plasma protein binding of drugs. *Annu. Rep. Med. Chem.* **1996**, *31*, 327–336.

(11) Qi, Z.-D.; Zhou, B.; Xiao, Q.; Shi, C.; Liu, Y.; Dai, J. Interaction of rofecoxib with human serum albumin: Determination of binding constants and the binding site by spectroscopic methods. *J. Photochem. Photobiol. A: Chem.* **2008**, *193*, 81–88.

(12) Peters, T., Jr. Serum Albumin. *Adv. Protein Chem.* **1985**, *37*, 161–245.

(13) Sasnouskia, S.; Zorin, V.; Khludeyev, I.; D'Hallewin, M.-A.; Guillemin, F.; Bezdetnaya, L. Investigation of Foscan interactions with plasma proteins. *Biochim. Biophys. Acta* **2005**, *1725*, 394–402.

(14) Hu, Y.-J.; Liu, Y.; Zhao, R.-M.; Dong, J.-X.; Qu, S.-S. Spectroscopic studies on the interaction between methylene blue and bovine serum albumin. *J. Photochem. Photobiol. A: Chem.* **2006**, *179*, 324–329.

(15) Simard, J. R.; Zunszain, P. A.; Ha, C. E.; Yang, J. S.; Bhagavan, N. V.; Petitpas, I.; Curry, S.; Hamilton, J. A. Locating high-affinity fatty acid-binding sites on albumin by x-ray crystallography and NMR spectroscopy. *Proc. Natl. Acad. Sci. U.S.A.* **2005**, *102*, 17958–17963.

(16) Spector, A. A. Fatty acid binding to plasma albumin. *J. Lipid Res.* **1975**, *16*, 165–179.

(17) Fredricson, D. S.; Gordon, R. S.; Ono, K.; Cherkes, A. The metabolism of albumin bound C14-labeled unesterified fatty acids in normal human subjects. *J. Clin. Invest.* **1958**, *37*, 1504–1515.

DOI: 10.1021/acs.jpcb.5b00965
J. Phys. Chem. B 2015, 119, 7804–7815

(18) Bhattacharya, A. A.; Grune, T.; Curry, S. Crystallographic analysis reveals common modes of binding of medium and long-chain fatty acids to human serum albumin. *J. Mol. Biol.* **2000**, *303*, 721−732.
(19) Ashbrook, J. D.; Spector, A. A.; Santos, E. C.; Fletcher, J. E. Long chain fatty acid binding to human plasma albumin. *J. Biol. Chem.* **1975**, *250*, 2333−2338.
(20) Kragh-Hansen, U.; Watanabe, H.; Nakajou, K.; Iwao, Y.; Otagiri, M. Chain length-dependent binding of fatty acid anions to human serum albumin studied by site-directed mutagenesis. *J. Mol. Biol.* **2006**, *363*, 702−712.
(21) Karush, F.; Sonenberg, M. Interaction of homologous alkyl sulfates with bovine serum albumin. *J. Am. Chem. Soc.* **1949**, *71*, 1369−1376.
(22) Cistola, D. P.; Small, D. M.; Hamilton, J. A. Medium-chain fatty acid binding to albumin and transfer to phospholipid bilayers. *J. Biol. Chem.* **1987**, *262*, 10971−10979.
(23) Cistola, D. P.; Small, D. M.; Hamilton, J. A. Carbon 13 NMR studies of saturated fatty acids bound to bovine serum albumin. II. Electrostatic interactions in individual fatty acid binding sites. *J. Biol. Chem.* **1987**, *262*, 10980−10985.
(24) Parks, J. S.; Cistola, D. P.; Small, D. M.; Hamilton, J. A. Interactions of the carboxyl group of oleic acid with bovine serum albumin: a 13C NMR study. *J. Biol. Chem.* **1983**, *258*, 9262−9269.
(25) Morrisett, J. D.; Pownall, H. J.; Gotto, A. M., Jr. Bovine serum albumin. Study of the fatty acid and steroid binding sites using spin-labeled lipids. *J. Biol. Chem.* **1975**, *250*, 2487−2494.
(26) Klotz, I. M.; Walker, F. M. The binding of organic ions by proteins. Charge and ph effects. *J. Am. Chem. Soc.* **1947**, *69*, 1609−1612.
(27) Ananthapadmanabhan, K. P. In *Interactions of Surfactants with Polymers and Proteins*, Goddard, E. D., Ananthapadmanabhan, K. P., Eds.; CRC Press, Inc.: London, U.K., 1993; Chapter 8.
(28) Moore, P. N.; Puvvada, S.; Blankschtein, D. Role of the surfactant polar head structure in protein−surfactant complexation: Zein protein solubilization by SDS and by SDS/C12En surfactant solutions. *Langmuir* **2003**, *19*, 1009−1016.
(29) Tadros, T. F. *Applied Surfactants: Principles and Applications*; Wiley-VCH verlag GmbH & Co.: Weinheim, 2005.
(30) Martinez, M. N.; Amidon, G. L. A mechanistic approach to understanding the factors affecting drug absorption: a review of fundamentals. *J. Clin. Pharmacol.* **2002**, *42*, 620−643.
(31) Jones, M. N. Surfactant interactions with biomembranes and proteins. *Chem. Soc. Rev.* **1992**, *21*, 127−136.
(32) Jones, M. N. In *Food Polymers, Gels and Colloids*; Dickenson, E., Ed.; The Royal Society of Chemistry: Cambridge, U.K., 1991; pp 65−80.
(33) McClements, D. J. *Food Emulsions: Principles, Practice and Techniques*, 2nd ed.; CRC Press: Boca Raton, FL, 2004.
(34) Moriyama, Y.; Takeda, K. Re-formation of the helical structure of human serum albumin by the addition of small amounts of sodium dodecyl sulfate after the disruption of the structure by urea. A comparison with bovine serum albumin. *Langmuir* **1999**, *15*, 2003−2008.
(35) Rozema, D.; Gellman, S. H. Artificial chaperones: Protein refolding via sequential use of detergent and cyclodextrin. *J. Am. Chem. Soc.* **1995**, *117*, 2373−2374.
(36) Foster, J. F. *Albumin Structure, Function and Uses*; Pergamon Press, Oxford, U.K., 1977.
(37) Papadopoulou, A.; Green, R. J.; Frazier, R. A. Interaction of flavonoids with bovine serum albumin: a fluorescence quenching study. *J. Agric. Food Chem.* **2005**, *53*, 158−163.
(38) He, X. M.; Carter, D. C. Atomic structure and chemistry of human serum albumin. *Nature* **1992**, *358*, 209−215.
(39) Dufour, C.; Dangles, O. Flavonoid-serum albumin complexation: determination of binding constants and binding sites by fluorescence spectroscopy. *Biochim. Biophys. Acta* **2005**, *1721*, 164−173.
(40) Singh, S. K.; Kishore, N. Thermodynamic insights into the binding of Triton X-100 to globular proteins: a calorimetric and spectroscopic investigation. *J. Phys. Chem. B* **2006**, *110*, 9728−9737.
(41) Ojha, B.; Das, G. The interaction of 5-(alkoxy)naphthalen-1-amine with bovine serum albumin and its effect on the conformation of protein. *J. Phys. Chem. B* **2010**, *114*, 3979−3986.
(42) Chakraborty, T.; Chakraborty, I.; Moulik, S. P.; Ghosh, S. Physicochemical and conformational studies on BSA-surfactant interaction in aqueous medium. *Langmuir* **2009**, *25*, 3062−3074.
(43) Ojha, B.; Das, G. Role of hydrophobic and polar interactions for BSA−amphiphile composites. *Chem. Phys. Lipids* **2011**, *164*, 144−150.
(44) Goddard, E. D. *Interaction of surfactant with polymers and proteins, Protein−Surfactant Interactions*; CRC Press: Boca Raton, FL, 1993.
(45) Tanford, C. *The Hydrophobic Effect: Formation of Micelles and Biological Membranes*, 2nd ed.; Wiley-Interscience: New York, 1980.
(46) de Sousa Neto, D.; Salmon, C. E. G.; Alonso, A.; Tabak, M. Interaction of bovine serum albumin (BSA) with ionic surfactants evaluated by electron paramagnetic resonance (EPR) spectroscopy. *Colloids Surf., B* **2009**, *70*, 147−156.
(47) Shingawa, S.; Sato, M.; Kameyama, K.; Takagi, T. Effect of salt concentration on the structure of protein-sodium dodecyl sulfate complexes revealed by small-angle x-ray scattering. *Langmuir* **1994**, *10*, 1690−1694.
(48) Turro, N. J.; Lei, X.-G.; Ananthapadmanabhan, K. P.; Aronson, M. Spectroscopic probe analysis of protein-surfactant interactions: The BSA/SDS System. *Langmuir* **1995**, *11*, 2525−2533.
(49) Guo, X. H.; Zhao, N. M.; Chen, S. H.; Teixeira, J. Small-angle neutron scattering study of the structure of protein/detergent complexes. *Biopolymers* **1990**, *29*, 335−346.
(50) Gelamo, E. L.; Silva, C. H.; Imasato, H.; Tabak, M. Interaction of bovine (BSA) and human (HSA) serum albumins with ionic surfactants: spectroscopy and modelling. *Biochim. Biophys. Acta* **2002**, *1594*, 84−99.
(51) Ding, Y.; Shu, Y.; Ge, L.; Guo, R. The effect of sodium dodecyl sulfate on the conformation of bovine serum albumin. *Colloids Surf., A* **2007**, *298*, 163−169.
(52) Tai, S.; Liu, X.; Chen, W.; Gaoa, Z.; Niu, F. Spectroscopic studies on the interactions of bovine serum albumin with alkyl sulfate gemini surfactants. *Colloids Surf., A* **2014**, *441*, 532−538.
(53) Mondal, S.; Das, S.; Ghosh, S. Interaction of myoglobin with cationic gemini surfactants in phosphate buffer at pH 7.4. *J. Surfact. Deterg.* **2015**, *18*, 471−476.
(54) Duggan, E. L.; Luck, F. M. The combination of organic anions with serum albumin: IV. Stabilization against denaturation. *J. Biol. Chem.* **1948**, *172*, 205−220.
(55) Moriyama, Y.; Kawasaka, Y.; Takeda, K. Protective effect of small amounts of sodium dodecyl sulfate on the helical structure of bovine serum albumin in thermal denaturation. *J. Colloid Interface Sci.* **2003**, *257*, 41−46.
(56) Moriyama, Y.; Watanabe, E.; Kobayashi, K.; Harano, H.; Inui, E.; Takeda, K. Secondary structural change of bovine serum albumin in thermal denaturation up to 130 degrees C and protective effect of sodium dodecyl sulfate on the change. *J. Phys. Chem. B* **2008**, *112*, 16585−16589.
(57) Moriyama, Y.; Takeda, K. Protective effects of small amounts of bis(2ethylhexyl)sulfosuccinate on the helical structures of human and bovine serum albumins in their thermal denaturations. *Langmuir* **2005**, *21*, 5524−5528.
(58) Ray, G. B.; Ghosh, S.; Moulik, S. P. Physicochemical studies on the interfacial and bulk behaviors of sodium n-dodecanoylsarcosinate (SDDS). *J. Surfact. Deterg.* **2009**, *12*, 131−143.
(59) Schmidt, R. R.; Fortna, R. H.; Beyer, H. H. European Patent, Application No. EP 0194097, 1986.
(60) Gad, E. A. M.; El-Sukkary, M. M. A.; Ismail, D. A. Surface and thermodynamic parameters of sodiumn-acyl sarcosinate surfactant solutions. *J. Am. Oil Chem. Soc.* **1997**, *74*, 43−47.

DOI: 10.1021/acs.jpcb.5b00965
J. Phys. Chem. B 2015, 119, 7804−7815

(61) De, M.; You, C.-C.; Srivastava, S.; Rotello, V. M. Biomimetic interactions of proteins with functionalized nanoparticles: A thermodynamic study. *J. Am. Chem. Soc.* **2007**, *129*, 10747−10753.
(62) Bordes, R.; Tropsch, J.; Holmberg, K. Role of an amide bond for self-assembly of surfactants. *Langmuir* **2010**, *26*, 3077−3083.
(63) Bajani, D.; Laskar, P.; Dey, J. Spontaneously formed robust steroidal vesicles: physicochemical characterization and interaction with HSA. *J. Phys. Chem. B* **2014**, *118*, 4561−4570.
(64) Roy, S.; Dey, J. Spontaneously formed vesicles of sodium n-(11-acrylamidoundecanoyl)-glycinate and l-alaninate in water. *Langmuir* **2005**, *21*, 10362−10369.
(65) Ghosh, A.; Dey, J. Effect of hydrogen bonding on the physicochemical properties and bilayer self-assembly formation of n-(2-hydroxydodecyl)-l-alanine in aqueous solution. *Langmuir* **2008**, *24*, 6018−6026.
(66) Ghosh, R.; Dey, J. Vesicle formation by l-cysteine-derived unconventional single-tailed amphiphiles in water: A fluorescence, microscopy, and calorimetric investigation. *Langmuir* **2014**, *30*, 13516−13524.
(67) Mhaskar, S. Y.; Prasad, R. B. N.; Laksminarayana, G. Synthesis of N-acyl amino acids and correlation of structure with surfactant properties of their sodium salts. *J. Am. Oil Chem. Soc.* **1990**, *67*, 1015−1019.
(68) Lakowicz, J. R. *Principles of Fluorescence Spectroscopy*; Plenum Press: New York, 1983.
(69) Bia, S.; Songa, D.; Tiana, Y.; Zhoua, X.; Liua, Z.; Zhanga, H. Molecular spectroscopic study on the interaction of tetracyclines with serum albumins. *Spectrochim. Acta, Part A* **2005**, *61*, 629−636.
(70) Zhang, H.-X.; Liu, E. Binding behaviour of DEHP to albumin: Spectroscopic investigation. *J. Inclusion Phenom. Macrocyclic Chem.* **2012**, *74*, 231−238.
(71) Moyna, Á.; Connolly, D.; Nesterenko, E.; Nesterenko, P. N.; Paull, B. Separation of selected transition metals by capillary chelation ion chromatography using acetyl-iminodiacetic acid modified capillary polymer monoliths. *J. Chromatogr. A* **2012**, *1249*, 155−163.
(72) Bordes, R.; Holmberg, K. Physical chemical characteristics of dicarboxylic amino acid-based surfactants. *Colloids Surf., A* **2011**, *391*, 32−41.
(73) Majorek, K. A.; Porebski, P. J.; Dayal, A.; Zimmerman, M. D.; Jablonska, K.; Stewart, A. J.; Chruszcz, M.; Minor, W. Structural and immunologic characterization of bovine, horse, and rabbit serum albumins. *Mol. Immunol.* **2012**, *52*, 174−182.
(74) Spector, A. A.; John, K. M. Effects of free fatty acid on the fluorescence of bovine serum albumin. *Arch. Biochem. Biophys.* **1968**, *127*, 65−71.
(75) Halfman, C. J.; Nishida, T. Nature of the alteration of the fluorescence spectrum of bovine serum albumin produced by the binding of dodecyl sulphate. *Biochim. Biophys. Acta* **1971**, *243*, 294.
(76) Reynolds, J.; Herbert, S.; Steinhardt, J. Binding of some long-chain fatty acid anions and alcohols by bovine serum albumin. *Biochemistry* **1968**, *7*, 1357−1367.
(77) Ping, M.; Yang, L.; Yezhong, Z.; Jiaxin, F.; Xiaohong, S.; Yi, L. Binding studies of a Schiff Base Compound containing a 1,2,4-triazole ring with bovine serum albumin using spectroscopic methods. *Chin. J. Chem.* **2010**, *28*, 1915−1922.
(78) Deep, S.; Ahluwalia, J. C. Interaction of bovine serum albumin with anionic surfactants. *Phys. Chem. Chem. Phys.* **2001**, *3*, 4583−4591.
(79) Spector, A. A.; John, K.; Fletcher, J. E. Binding of long-chain fatty acids to bovine serum albumin. *J. Lipid Res.* **1969**, *10*, 56−67.
(80) Spector, A. A.; Fletcher, J. E.; Ashbrook, J. D. Analysis of long-chain free fatty acid binding to bovine serum albumin by determination of stepwise equilibrium constants. *Biochemistry* **1971**, *10*, 3229−3232.
(81) Anand, U.; Jash, C.; Mukherjee, S. Spectroscopic probing of the microenvironment in a protein-surfactant assembly. *J. Phys. Chem. B* **2010**, *114*, 15839−15845.
(82) Samanta, A.; Paul, B. K.; Guchhait, N. Spectroscopic probe analysis for exploring probe−protein interaction: A mapping of native, unfolding and refolding of protein bovine serum albumin by extrinsic fluorescence probe. *Biophys. Chem.* **2011**, *156*, 128−139.
(83) Syme, N. R.; Dennis, C.; Bronowska, A.; Paesen, G. C.; Homans, S. W. Comparison of entropic contributions to binding in a "hydrophilic" versus "hydrophobic" ligand−protein interaction. *J. Am. Chem. Soc.* **2010**, *132*, 8682−8689.

DOI: 10.1021/acs.jpcb.5b00965
J. Phys. Chem. B 2015, 119, 7804−7815